Plasma-Immersion Ion Implantation of the Interior Surface of a Small Cylindrical Bore Using an Auxiliary Electrode for Finite Rise-Time Voltage Pulses

Xuchu Zeng, Tat-Kun Kwok, Aiguo Liu, Paul K. Chu, Baoyin Tang, and Terrence E. Sheridan

***Abstract*— Plasma-immersion ion implantation (PIII) can be used to process the interior surfaces of odd-shape specimens such as a cylindrical bore. The temporal evolution of the plasma sheath in a small cylindrical bore in the presence of a grounded coaxial auxiliary electrode is derived for voltage pulses of different rise times by solving Poisson's equation and the equations of ion continuity, and motion numerically using the appropriate boundary conditions. It is found that the maximum ion impact energy and the average impact energy are improved for finite rise-time voltage pulses, and shorter rise times yield better results. Our results allow the selection of a suitable auxiliary electrode radius to improve the average impact energy for a given rise time.**

***Index Terms*— Ion implantation, plasma applications, plasma sheath.**

I. Nomenclature

D	Ion–matrix overlap radius.
n_0	Uniform ion density.
n_i	Ion density.
ϕ	Unknown potential.
ϕ_t	Target bias.
ϕ_p	Peak voltage of the pulse.
ε_0	Permittivity of free space.
e	Charge of electron.
r_b	Radius of the cylindrical bore.
r_a	Radius of the auxiliary electrode.
r	Radial coordinate.
T_e	Temperature of electron.
M	Ion mass.
$v_i(0)$	Initial ion velocity.
v_i	Ion velocity.
t	Temporal coordinate.
t_r	Rise time of the voltage pulse.
k	Boltzmann constant.
ρ	Normalized radial coordinate.
ρ_b	Normalized radius of the cylindrical bore.
ρ_a	Normalized radius of the auxiliary electrode.
Ψ	Normalized unknown potential.
Ψ_t	Normalized target bias.
N_i	Normalized ion density.
V_i	Normalized ion velocity.
T	Normalized temporal coordinate.
T_r	Normalized rise time of the voltage pulse.
$v_{\max}$	Maximum ion velocity.
ω_{pi}	Ion plasma frequency.
h	Grid size in space.
f	Time step.
i	Discrete space coordinate.
j	Discrete temporal coordinate.
c	Constant.
E_{it}	Normalized ion impact energy.
$E_{t\max}$	Maximum normalized ion impact energy.
$E_{t\text{avg}}$	Average normalized ion impact energy.
$f(E_{it})$	Ion impact energy-distribution function.

Manuscript received June 25, 1997; revised January 5, 1998. The work was supported by the Hong Kong Research Grants Council under Central Allocation Grant 8730005, by the Hong Kong Research Grants Council under Earmark Grants 9040220 and 9040332, and by the City University of Hong Kong under Strategic Research Grant 7000730.

X. Zeng, T.-K. Kwok, A. Liu, P. K. Chu, and B. Tang are with the Department of Physics and Materials Science, City University of Hong Kong, Kowloon, Hong Kong (e-mail: appkchu@cityu.edu.hk).

T. E. Sheridan is with the Plasma Research Laboratory, Australian National University, Canberra, A.C.T. 0200, Australia.

Publisher Item Identifier S 0093-3813(98)02722-2.

II. Introduction

PLASMA-IMMERSION ion implantation (PIII) is an innovative and fledgling technique to enhance the surface properties of materials such as metals, polymers, ceramics, and semiconductors [1]–[3]. An appealing feature of PIII is that it is possible to implant surfaces that are not line-of-sight accessible. Interior surfaces of industrial components such as dies, bushings, pipes, and piston rings pose a formidable challenge to conventional ion-beam implantation techniques, and so the problems of inner surface modification using PIII have attracted the attention of physicists and materials scientists [4]–[11].

The structure of the ion–matrix sheath in a transitionally invariant cylindrical bore has been investigated [4], and the crucial parameter is the ion–matrix overlap radius D which is

given by the following relationship:

$$D = \sqrt{\frac{-4\varepsilon_0 \phi_t}{e n_0}} \tag{1}$$

where n_0 is the uniform ion density and ϕ_t is the target bias. For zero rise-time voltage pulses and when the radius of a cylindrical bore r_b is less than or equal to D, the bore is filled by an unneutralized ion component, and can be categorized as a "small bore case." When r_b is larger than D, there is a region of neutral plasma around the axis and it is referred to as a "large bore case." Previous studies have concluded that for PIII in a cylindrical bore, improving the impact energy is most crucial, especially for a small bore [5], [6].

We have proposed to increase the impact energy of ions implanted into the interior sidewalls of cylindrical specimens by using an auxiliary electrode [11], [12]. The ion–matrix sheath and temporal evolution of the ion–matrix sheath in a small cylindrical bore have been calculated for zero rise-time voltage pulses, and the impact energy increases significantly in the presence of an auxiliary electrode. However, even though our previous results provide the theoretical foundation, zero rise-time voltage pulses are unrealistic and further investigation must be carried out to incorporate finite rise-time voltage pulses to simulate real experimental conditions. In this paper, our work is focused on the effects of finite rise-time voltage pulses. In this scenario, it can no longer be assumed that there are only ions in the bore and the electron distribution, and the expansion of the plasma sheath in the bore must be considered together.

III. Fluid Modeling and Formalism

We consider PIII into the interior sidewall of a cylindrical bore with an auxiliary electrode, as shown schematically in Fig. 1. The radius of the bore is $r_b (r_b \leq D)$ and the radius of the auxiliary electrode is $r_a (r_a < r_b)$. The variable r measures the distance from the symmetry axis. The system is transitionally invariant along the axis of the bore, and it is azimuthally symmetrical, so that the variables only depend on r. When $(r_b - r_a)$ is more than the Debye length, we assume that the bore is essentially uniformly filled with a neutral plasma in which the density of electrons and ions are both n_0 and the potential is zero. The electron is characterized by the electron temperature T_e. The ion mass is M and the ion charge is e. The initial ion velocity $v_i(0)$ is zero and the potential in the bore is given by [13], [14]

$$\phi_t = \begin{cases} \phi_p (t/t_r), & t \leq t_r \\ \phi_p, & t > t_r. \end{cases} \tag{2}$$

It is important to point out that the effects of the fall time of the voltage pulse is negligible as a pulse of sufficient duration will deplete almost all the ions within the bore and there are practically no ions left to experience the fall [6].

This situation is modeled using cold collisionless fluid ions, Boltzmann electrons, and Poisson's equation [15]. In cylindrical coordinates, the equations of ion continuity and

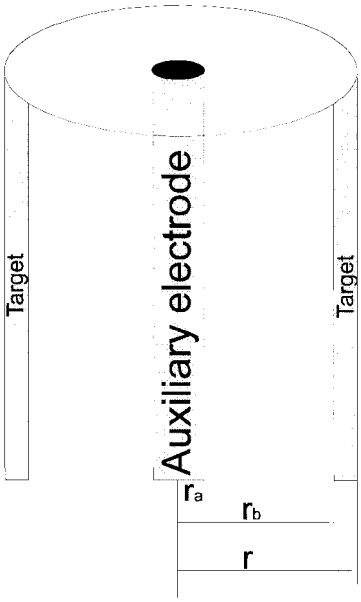

Fig. 1. Schematic of the problem considered. The plasma with a uniform ion density n_0 initially fills the space between a cylindrical bore and an auxiliary electrode. The radius of the bore is r_b and its potential is $\phi_t (\phi_t < 0)$. The radius of the conductive auxiliary electrode is r_a and its potential is zero.

motion, Boltzmann's relationship, and Poisson's equation are

$$\frac{\partial n_i}{\partial t} + \frac{1}{r}\frac{\partial}{\partial r}(r n_i v_i) = 0 \tag{3}$$

$$\frac{\partial v_i}{\partial t} + v_i \frac{\partial v_i}{\partial r} = -\frac{e}{M}\frac{\partial \phi}{\partial r} \tag{4}$$

$$n_e = n_0 \exp(e\phi / K T_e) \tag{5}$$

$$\frac{1}{r}\frac{\partial}{\partial r} r \frac{\partial \phi}{\partial r} = -\frac{e}{\varepsilon_0}(n_i - n_e) \tag{6}$$

where $0 < r_a \leq r \leq r_b \leq D$. The variables can be made dimensionless by normalization. The dimensionless variables used in this work are

$$\rho = \frac{r}{D} \quad \Psi = \frac{\phi}{\phi_p} \quad N_i = \frac{n_i}{n_0} \quad V_i = \frac{v_i}{v_{\max}} \quad T = t\omega_{pi} \tag{7}$$

where $v_{\max} = \sqrt{-2e\phi_p / M}$ is the velocity the ion would have if it fell through a potential drop ϕ_p, and $\omega_{pi} = \sqrt{n_0 e^2 / \varepsilon_0 M}$ is the ion plasma frequency. In this way, the radius of the bore and the auxiliary electrode are $\rho_b = r_b / D$ and $\rho_a = r_a / D$, respectively. After substituting (5) into (6), the equations become

$$\frac{\partial N_i}{\partial T} + \frac{1}{\sqrt{2}}\frac{1}{\rho}\frac{\partial}{\partial \rho}(\rho N_i V_i) = 0 \tag{8}$$

$$\frac{\partial V_i}{\partial T} + \frac{1}{\sqrt{2}} V_i \frac{\partial V_i}{\partial \rho} = \frac{1}{2\sqrt{2}}\frac{\partial \Psi}{\partial \rho} \tag{9}$$

$$\frac{1}{\rho}\frac{\partial}{\partial \rho}\rho \frac{\partial \Psi}{\partial \rho} = 4(N_i - \exp(e\phi_p \Psi / K T_e)) \tag{10}$$

where $0 < \rho_a \leq \rho \leq \rho_b \leq 1$. Equation (2) also becomes

$$\Psi_t = \begin{cases} T/T_r, & T \leq T_r \\ 1, & T > T_r \end{cases} \tag{11}$$

where $T_r = t_r \omega_{pi}$ is the dimensionless rise time.

Equations (8)–(10) are solved by finite-difference methods. The discrete finite-difference equations in the presence of an auxiliary electrode are

$$N_{i,j+1} = N_{i,j} - \frac{f}{\sqrt{2}h(\rho_a+ih)} \cdot [hN_{i,j}V_{i,j}+(\rho_a+ih)(2N_{i,j}v_{i,j}-N_{i,j}V_{i-1,j} -N_{i-1,j}V_{i,j})] \tag{12}$$

$$V_{i,j+1} = V_{i,j}+\frac{f}{2\sqrt{2}h}[(\Psi_i-\Psi_{i-1})-2(V_{i,j})^2+2V_{i,j}V_{i-1,j}] \tag{13}$$

$$\Psi_{i+1}(\rho_a+ih)+\Psi_i(h-2ih-2\rho_a)+\Psi_{i-1}(\rho_a+ih-h) = 4h^2(\rho_a+ih)(N_{i,j}-\exp(-c\Psi_i)) \tag{14}$$

where $c = (e|\phi_P|/KT_e), h$ is the grid size in space, i.e., $\rho_{i+1}-\rho_i = h, f$ is the time step used in our iteration, i.e., $T_{j+1}-T_j = f$, and i and j are positive integers. $N_{i,j}$, $V_{i,j}$, and Ψ_i are the normalized ion density, ion velocity, potential at normalized radii $\rho = \rho_a+ih$, and time $T = jf$, respectively. Note that the normalized potential Ψ is not a direct function of T except at the target, and only N and V are partially differentiated with respect to T, as shown in (9) and (10). However, Ψ will indeed change with time as N will vary with T as indicated in (10) and (14). The boundary conditions are: $\Psi_0 = 0$ and $N_{0,j} = 0$ at $\rho = \rho_a$, and $\Psi_{(\rho_b-\rho_a)/h} = \Psi_t$ at $\rho = \rho_b$. The initial conditions are: $\Psi_i = 0$, $V_{i,0} = 0$, $N_{i,0} = 1$ for $i > 0$.

Equation (14) is solved via numerical iteration by first letting ϕ be an initial solution and linearizing (14) about this value using [16]

$$\exp(-c\Psi) = \exp(-c\phi)\exp(-c(\Psi-\phi)) = \exp(-c\phi)(1-c\Psi+c\phi). \tag{15}$$

After neglecting higher order terms, (15) becomes (16), shown at the bottom of the page. We take ϕ from ψ of the previous time step, solve (16) to obtain a new ψ, set ϕ equal to this new ψ, and iterate until the process converges. Typically, it takes two–three iterations to converge.

The solved potential Ψ_i is then used to determine the normalized ion velocity $V_{i,j+1}$ and ion density $N_{i,j+1}$ of the next time step $j+1$ using (12) and (13). The process of solving the potential at a time step as well as determining the ion velocity and ion density at the next time step is continued until the end of the simulation. A mesh of 200 grids in space and a time step $f = 0.001$ is used in my simulation. Therefore, h is equal to (1.0-0.1)/200 or 0.0045 when an auxiliary electrode is present ($\rho_a = 0.1$). For $|\Phi_p| = 50$ kV and $kT_e = 5$ eV, c is equal to 10^4.

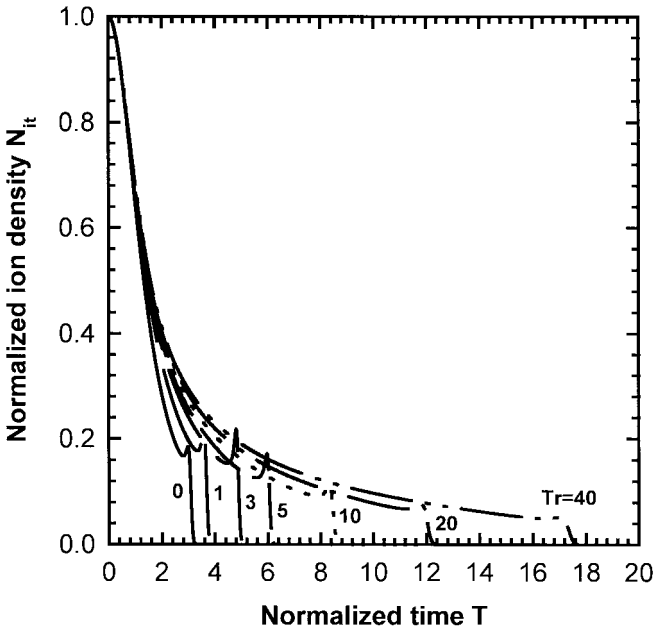

Fig. 2. Time dependence of the normalized ion density N_{it} at the target surface ($\rho = \rho_b = 1$) for dimensionless rise times $T_r = 0$, 1, 3, 5, 10, 20, and 40. The dimensionless variables are described in (7) and $\rho_a = 0.1$.

IV. Results and Discussion

To study the finite rise-time effects, the radii of the bore and the auxiliary electrode are first fixed at $\rho_b = 1$ and $\rho_a = 0.1$, and the rise time is varied ($T_r = 0$, 1, 3, 5, 10, 20, and 40). The results by the fluid model for $T_r = 0$ (zero rise time) are first compared to our previously reported solutions [12] and agree to better than 0.1%. The fluid model results in the case without the auxiliary electrode are generated for $T_r = 20$ and 40 and compared to the results in the literature [6]. The agreement is found to be better than 0.2%. In order to further corroborate our model and algorithm, simulation is also carried out by the particle-in-cell (PIC) method. In the PIC study, the grid spacing is 0.25 Debye length, the time step is 1/256 ω_{pi}^{-1}, and 64 ion particles are used in each cell initially. The results generated by these two distinctly different methods are consistent, thereby confirming the validity of the fluid model.

The relationship between the dimensionless ion density at the target N_{it} and the rise time is displayed in Fig. 2. In all cases, there is a steep initial decay in the target ion density, but the rate of decrease slows down as the sheath propagates across the bore. Finally, the faster ions catch up to the slower ones to give rise to the peaks, and N_{it} then decreases precipitously to zero. It is obvious that the time needed to deplete all ions increases with T_r. It can also be observed that for a large rise time, e.g., $T_r \geq 10$, the ions are exhausted when the potential at the target reaches the plateau value. Based on our results, the peak attains the maximum value when $T_r = 3$. It indicates that the ions close to the auxiliary electrode are accelerated

$$\Psi_{i+1}(\rho_a+ih)+\Psi_i(h-2ih-2\rho_a-4h^2(\rho_a+ih)c\exp(-c\phi))+\Psi_{i-1}(\rho_a+ih-h) = 4h^2(\rho_a+ih)(N_{i,j}-\exp(-c\phi)-c\phi\exp(-c\phi)). \tag{16}$$

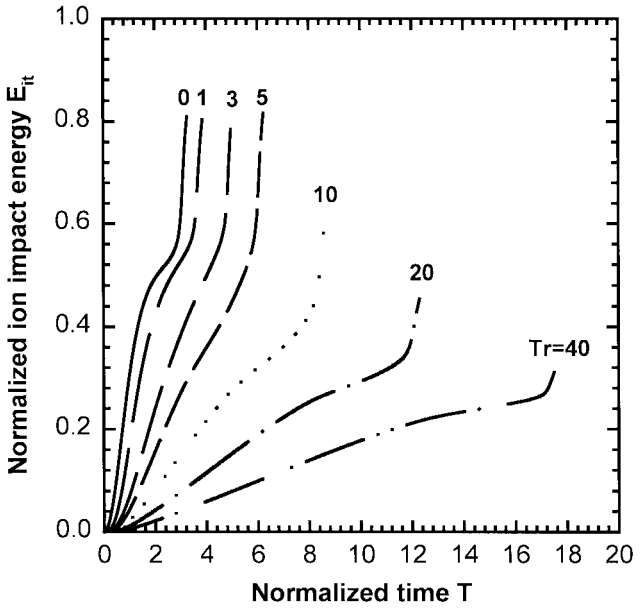

Fig. 3. Normalized ion impact energy E_{it} versus normalized time T for normalized rise times $T_r = 0$, 1, 3, 5, 10, 20, and 40. The dimensionless variables are described in (7), $\rho_a = 0.1$ and $\rho_b = 1.0$.

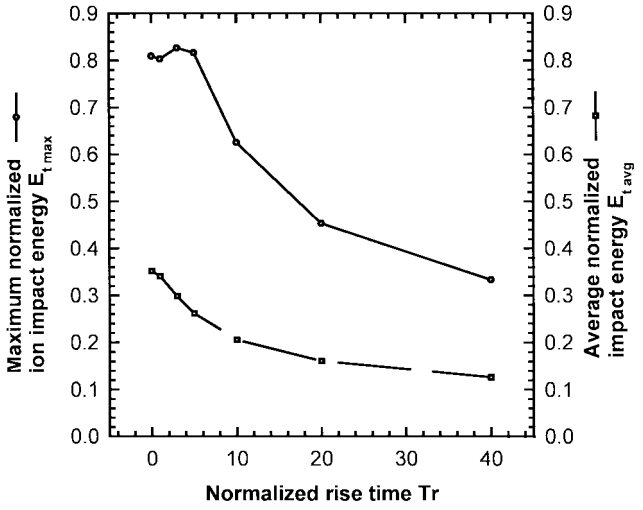

Fig. 4. Rise-time dependence of the normalized maximum ion impact energy $E_{t\max}$ and the normalized average ion impact energy $E_{t\text{avg}}$. The dimensionless variables are described in (7), $\rho_a = 0.1$ and $\rho_b = 1.0$.

better, and thus more ions are able to catch up to the slower ones. This point can be verified by observing the normalized ion impact energy E_{it} for the different rise times, as exhibited in Fig. 3. The normalized ion impact energy is given by

$$E_{it} = \frac{\frac{1}{2}Mv_{it}^2}{-e\phi_p} = \frac{\frac{1}{2}Mv_{it}^2}{\frac{1}{2}Mv_{\max}^2} = V_{it}^2. \tag{17}$$

Here, v_{it} is the ion velocity at the target. As the ions are initially at rest, the impact energy starts at zero, increases monotonically with time, and finally reaches the maximum. This is very different from the case without the auxiliary electrode, in which case the impact energy decays after the sheath reaches the axis [6]. It is interesting to note that the maximum ion impact energy is not achieved at $T_r = 0$, but rather at $T_r = 3$. This point is further illustrated in Fig. 4, which depicts the maximum normalized ion impact energy $E_{t\max}$ and the average normalized ion impact energy $E_{t\text{avg}}$, i.e., implant energy per ion for different T_r. For $\rho_b = 1$ and $\rho_a = 0.1$, it is found that the ions near the auxiliary electrode will get the maximum ion impact energy because they experience a longer accelerating time and a bigger average accelerating electric field. The effects of the rise time T_r on the maximum ion impact energy can be visualized in two ways. The electric field between the bore and the auxiliary electrode increases rapidly for a short T_r and, consequently, the maximum ion impact energy is improved. On the other hand, the electric field is bunched near the target, and because many ions are still in the bore for a short T_r, the benefits to the maximum ion impact energy are not as substantial. Hence, the ion impact energy does not peak at $T_r = 0$, but at $T_r = 3$. As shown in Fig. 4, the difference of the maximum ion impact energy is small for $T_r = 0$–5. The average impact energy goes up with decreasing rise time because the faster rise time accelerates the majority of the ions better. It can be observed that the decay rate of the average impact energy is larger in the range $0 < T_r < 5$ than when $T_r > 5$ and becomes very mild at $T_r > 20$. We believe that there are still some ions which will acquire better acceleration in the bore when the voltage pulse reaches the plateau for $0 < T_r < 5$. The shorter T_r implies that more ions get better acceleration and so the decay rate of the average impact energy is steep. When the rise time is large, the ions have already been depleted from the bore as the voltage pulse reaches the plateau. A larger T_r matches a larger ion depletion time (Fig. 2) and it implies that some ions can still be accelerated even though the voltage pulse rises slowly. Thus, the average impact energy is not sensitive to the rise time when $T_r > 10$.

In order to understand the ion energy distribution, the time-integrated ion impact energy distribution function $f(E_{it})$ for different values of T_r are plotted in Fig. 5, where the distribution is normalized such that the integral over the impact energy gives the total normalized dose. The population of energetic ions is larger for a shorter T_r. This is because the accelerating electric field increases very rapidly for a small rise time and more ions experience better acceleration.

In order to study the rise-time effects for different auxiliary electrode radii, we have performed the simulation for $\rho_a = 0$ (without an auxiliary electrode), 0.2, and 0.5. Fig. 6 plots the normalized average ion impact energy $E_{t\text{avg}}$ versus rise time T_r for $\rho_a = 0$, 0.2, and 0.5. It can be observed that when the rise time is short, the average ion impact energy can be enhanced by using a larger auxiliary electrode, but not so for a longer rise time. When T_r and ρ_a are large, the average ion impact energy is in fact smaller than that when there is no auxiliary electrode ($\rho_a = 0$). When T_r is small, there are still a copious number of ions within the bore when the bias has plateaued, and the average ion impact energy depends primarily on the strength and uniformity of the electric field between the bore and the auxiliary electrode. Because the electric field is larger and more uniform for a larger ρ_a, the average impact energy is naturally higher for a larger auxiliary electrode radius. On the contrary, when T_r is long,

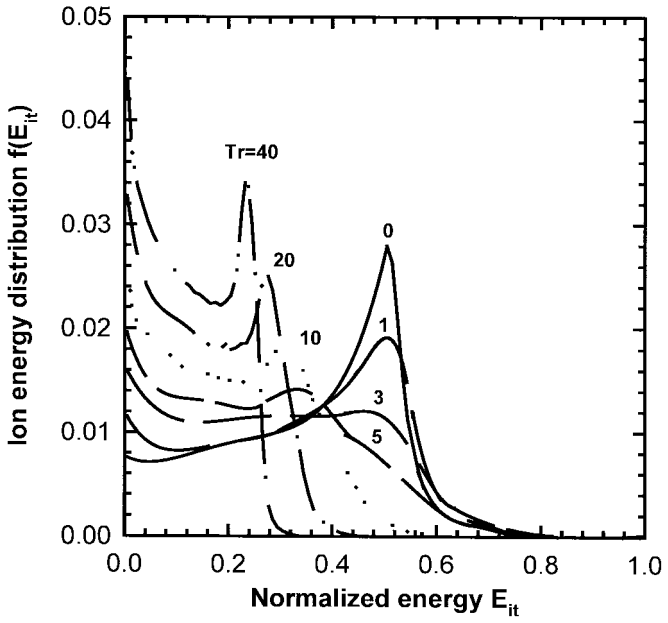

Fig. 5. The time-averaged ion energy distribution $f(E_{it})$ at the target ($\rho = \rho_b = 1$ and $\rho_a = 0.1$) for dimensionless rise times $T_r = 0, 1, 3, 5, 10, 20,$ and 40. All the distributions are normalized to give the total dose.

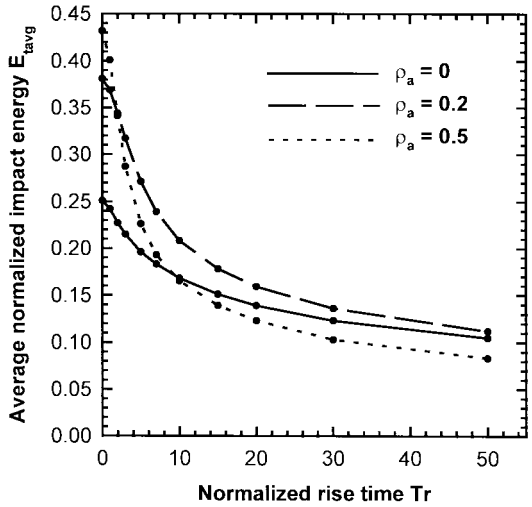

Fig. 6. Normalized average ion impact energy $E_{t\mathrm{avg}}$ versus normalized rise time T_r for $\rho_a = 0$, 0.2, and 0.5, and $\rho_b = 1.0$. The dimensionless variables are described in (7).

most of the ions have already depleted from the bore before the voltage pulse plateaus, and the average impact energy is mainly dependent on the average potential before the ions are depleted. The smaller the auxiliary electrode radius, the larger is the spacing between the auxiliary electrode and the interior surface of the cylindrical bore sample, and the longer time the ions will have to experience the accelerating electric field. In addition, the accelerating voltage is continuously increasing until the plateau and ions which remain in the bore longer (i.e., smaller ρ_a) will attain a higher net-impact energy. Hence, the average impact energy is larger for a smaller auxiliary electrode radius when T_r is long. Consequently, the choice of the electrode radius depends on the rise time of the pulsing electronics and, in general, a smaller ρ_a is preferred for a reasonable rise time.

V. Conclusion

The maximum ion impact energy and the average energy are enhanced by using a grounded auxiliary electrode positioned along the central axis of a cylindrical bore sample for the more realistic finite rise-time voltage pulses. For example, consider a maximum target bias of -100 kV applied to a cylindrical bore with a radius equal to the ion–matrix overlap length ($\rho_b = 1$). If an auxiliary electrode is used ($\rho_a = 0.1$) and $T_r = 5$, the maximum ion impact energy is 82 kV and the average impact energy is 26 kV. However, in the absence of the auxiliary electrode and $T_r = 5$, the values will be 33 and 19 kV, respectively. When the rise time is lengthened to $T_r = 40$, the effects of the auxiliary electrode are not as pronounced. For instance, the maximum ion impact energy changes from 34 to 22 kV and the average impact energy drops from 11.3 to 11 kV. Our results thus suggest that a faster voltage rise time is essential to attain good ion impact energy. When a high slew-rate pulsing power supply is not available, the choice of the auxiliary electrode becomes important, as a smaller radius does not necessarily give rise to high impact energy. Our model provides a means to calculate the best auxiliary electrode radius for a given rise time in order to achieve the maximum average ion impact energy.

References

[1] J. R. Conrad, J. L. Radtke, R. A. Dodd, F. J. Worzala, and N. C. Tran, "Plasma source ion implantation technique for surface modification of materials," *J. Appl. Phys.*, vol. 62, pp. 4591–4596, 1987.

[2] P. K. Chu, S. Qin, C. Chan, N. W. Cheung, and L. A. Larson, "Plasma immersion ion implantation—A fledgling technique for semiconductor processing," *Mater. Sci. Eng.*, vol. R17, no. 6–7, pp. 207–280, 1996.

[3] J. V. Mantese, I. G. Brown, N. W. Cheung, and G. A. Collins, "Plasma-immersion ion implantation," *MRS Bull.*, vol. 21, no. 8, pp. 52–56 1996.

[4] T. E. Sheridan, "Ion–matrix sheath in a cylindrical bore," *J. Appl. Phys.*, vol. 74, no. 8, pp. 4903–4906, 1993.

[5] ——, "Pulsed sheath dynamics in a small cylindrical bore," in *Physics of Plasmas*, vol. 1. New York: AIP, 1994, pp. 3485–3489.

[6] ——, "Transient sheath in a cylindrical bore for finite rise-time voltage pulses," *Surf. Coatings Technol.*, vol. 85, pp. 204–208, 1996.

[7] ——, "Sheath expansion into a large bore," *J. Appl. Phys.*, vol. 80, no. 1, pp. 66–69, 1996.

[8] M. Sun, S. Z. Yang, B. Li, and X. C. Chen, "Inner surface modification of 40 Cr steel cylinder with plasma source ion implantation," *J. Vac. Sci. Technol.*, to be published.

[9] M. Sun and S. Yang, "Measurements of spatial and temporal sheath evolution inside tubular material for inner surface ion implantation," *J. Vac. Sci. Technol. A, Vac. Surf. Films*, vol. 14, no. 6, pp. 3071–3074, 1996.

[10] M. Sun, S. Yang, and B. Li, "New method of tubular material inner surface modification by plasma source ion implantation," *J. Vac. Sci. Technol. A, Vac. Surf. Films*, vol. 14, no. 2, pp. 367–369, 1996.

[11] X. C. Zeng, B. Y. Tang, and P. K. Chu, "Improving the plasma immersion ion implantation impact energy inside a cylindrical bore by using an auxiliary electrode," *Appl. Phys. Lett.*, vol. 69, no. 25, pp. 3815–3817, 1996.

[12] X. C. Zeng, A. G. Liu, T. K. Kwok, P. K. Chu, and B. Y. Tang, "Pulsed sheath dynamics in a small cylindrical bore with an auxiliary electrode," *Phys. Plasma*, vol. 4, no. 12, pp. 4431–4434, 1997.

[13] I. T. Scheuer, M. Shamin, and J. R. Conrad, "Model of plasma source ion implantation in planar, cylindrical, and spherical geometries," *J. Appl. Phys.*, vol. 67, pp. 1241–1245, 1990.

[14] R. A. Stewart and M. A. Lieberman, "Model of plasma immersion ion implantation for voltage pulses with finite rise and fall times," *J. Appl. Phys.*, vol. 70, pp. 3481–3487, 1991.
[15] M. Widner, I. Alexeff, W. D. Jones, and K. E. Lonngren, "Ion acoustic wave excitation and ion sheath evolution," *Phys. Fluids*, vol. 13, no. 10, pp. 2532–2540, 1970.
[16] G. A. Emmert and M. A. Henry, "Numerical simulation of plasma sheath expansion, with applications to plasma-source ion implantation," *J. Appl. Phys.*, vol. 71, no. 1, pp. 113–117, 1992.

Xuchu Zeng was born in Sichuan, China, on February 12, 1964. He received the B.S. degree in electrical engineering from Xian JiaoTong University, China, in 1985 and the M.S. degree in plasma physics from the Southwestern Institute of Physics, China, in 1991. He is currently pursuing the Ph.D. degree at the City University of Hong Kong, China.

He was appointed Assistant Engineer, Engineer, and Senior Engineer in 1986, 1992, and 1994, respectively, at the Southwestern Institute of Physics. From June 1995 to June 1997 he was a Research Staff Member of the Plasma Laboratory, City University of Hong Kong. His research interests include plasma immersion ion implantation equipment design, as well as applications.

Tat-Kun Kwok received the B.Sc. degree in physics in 1988 and the Ph.D. degree in solid state physics in 1993 from King's College London, University of London, U.K.

From 1994 to 1995 he served as a Postdoctoral Fellow at the Surface Physics Lab, Fudan University, Shanghai, China. From 1995 to 1996 he was a Research Associate with the Physics Department, Hong Kong University of Science and Technology, Hong Kong. Currently, he is a Research Fellow, Department of Physics and Materials Science, City University of Hong Kong. He has published papers on topics related to photoluminescence and photo-absorption of point defects in silicon, reflectance difference spectroscopy, and numerical simulation of plasma immersion ion implantation.

Aiguo Liu was born in 1969. He received the B.S. and M.S. degrees in material science and technology from Harbin Institute of Technology, China, in 1991 and 1994, respectively. He is currently pursuing the Ph.D. degree at the Harbin Institute of Technology.

From June 1996 to December 1997, he served as a Research Assistant with the Plasma Laboratory, City University of Hong Kong, Hong Kong. While there, he was responsible for the control system of the plasma immersion ion implanter. His current research interests include plasma processing, metal material modification, and low-temperature plasma simulation.

Paul K. Chu received the B.S. degree in mathematics from The Ohio State University, Columbus, in 1977 and the M.S. and Ph.D. degrees in chemistry from Cornell University, Ithaca, NY, in 1979 and 1982, respectively.

He held various technical and managerial positions at Charles Evans & Associates in California from 1982 to 1990. He founded Evans Asia in 1990. He is currently a Professor with the Department of Physics and Materials Science, City University of Hong Kong, Hong Kong. He also holds concurrent professorship at Fudan University and Peking University, Beijing, China. His research interests include plasma immersion ion implantation, electronic materials, and materials characterization.

Baoyin Tang graduated from the Department of Engineering Physics, Harbin Institute of Technology, China, in 1960.

Prior to 1990, he was engaged in teaching works on electrical physics and research works on accelerators, ion sources, and ion implantation. From April 1990 to December 1992, he was with the Plasma Source Ion Implantation Group, University of Wisconsin-Madison, studying plasma-based ion implantation and surface modification of advanced materials. Since 1995, he has been working with Prof. P. K. Chu at the Department of Physics and Materials Science, City University of Hong Kong, Hong Kong. Currently, he is a Professor and Director of the Surface Modification of Materials Group in the Advanced Welding and Production Technology National Key Lab, Harbin Institute of Technology. His research works include development of multipurpose PIII equipment, improvement of PIII techniques, and industrial applications. In recent years, he has published more than 40 scientific and technical papers in international conferences and journals.

Terrence E. Sheridan received the B.A. degree in physics from Hiram College, Hiram, OH, in 1983 and the Ph.D. degree in plasma physics from Dartmouth College, Hanover, NH, in 1987.

He held postdoctoral appointments at the University of Iowa, Iowa City, and West Virginia University, Morgantown, and has taught at Glenville State College, Glenville, WV. He currently holds a research fellowship in the Space Plasma and Plasma Processing Group at the Australian National University, Canberra, Australia. His research interests include experimental characterization and simulation of sputtering magnetron discharges, dusty plasmas, plasma sheath dynamics (particularly the interior problem and two-dimensional targets), and the theory and modeling of ion-acoustic solitons. He has authored more than 50 publications.